Band structure and itinerant magnetism in quantum critical $NbFe_2$

Alaska Subedi
Department of Physics and Astronomy, University of Tennessee, Knoxville, Tennessee 37996, USA
and Materials Science and Technology Division, Oak Ridge National Laboratory, Oak Ridge, Tennessee 37831-6114, USA

David J. Singh
Materials Science and Technology Division, Oak Ridge National Laboratory, Oak Ridge, Tennessee 37831-6114, USA
(Received 20 November 2009; revised manuscript received 7 January 2010; published 26 January 2010)

We report first-principles calculations of the band structure and magnetic ordering in the C14 Laves phase compound $NbFe_2$. The magnetism is itinerant in the sense that the moments are highly dependent on ordering. We find an overestimation of the magnetic tendency within the local spin-density approximation, similar to other metals near magnetic quantum critical points. We also find a competition between different magnetic states due to band-structure effects. These lead to competing magnetic tendencies due to competing interlayer interactions, one favoring a ferrimagnetic solution and the other an antiferromagnetic state. While the structure contains Kagome lattice sheets, which could, in principle, lead to strong magnetic frustration, the calculations do not show dominant nearest-neighbor antiferromagnetic interactions within these sheets. These results are discussed in relation to experimental observations.

DOI: 10.1103/PhysRevB.81.024422 PACS number(s): 75.10.Lp, 71.20.Lp, 75.50.Bb

I. INTRODUCTION

There has been considerable recent interest in metals near magnetic quantum critical points (QCPs) both because new ground states such as superconductivity and nematic phases that have been reported in some as well as improved materials preparation and experimental techniques that allow detailed characterization of these phases including the unusual scalings of properties near the critical point.[1] Iron compounds are of particular interest because of the recent discovery of high-temperature superconductivity in iron compounds near magnetism,[2] with a possibly magnetic pairing mechanism.[3]

The hexagonal C14 hexagonal Laves phase compound $NbFe_2$ was thought to be either paramagnetic or very weakly ferromagnetic until 1987.[4,5] However, nuclear-magnetic-resonance (NMR) experiments by Yamada and Sakata found $NbFe_2$ to be a weak antiferromagnet with $T_N \sim 10$ K and $M \sim 0.1\mu_B$.[6] The antiferromagnetic state is very sensitive to stoichiometry and the material becomes ferromagnetic by slight over doping of either Nb or Fe, indicating the existence of a QCP at or very close to stoichiometric $NbFe_2$. The proximity to quantum criticality is also seen in the non-Fermi-liquid behavior of specific-heat capacity and resistivity. Wada *et al.*[7] reported that the electronic specific heat is substantially enhanced and more recently it was found that the Sommerfeld coefficient in fact shows logarithmic dependence $\gamma \propto -\log T$ at low temperatures.[8–11] The low-temperature resistivity meanwhile shows a behavior $\rho \propto T^{3/2}$. Furthermore, $NbFe_2$ shows a substantial exchange splitting of the Fe 3*s* core level, in spite of having a very low ordered moment.[12] This is a feature shared in common with the iron-based superconductors.[13]

$NbFe_2$ has the hexagonal C14 structure with Nb at $4f(1/3,2/3,x)$ and Fe at $2a(0,0,0)$ and $6h(y,2y,3/4)$. A unit cell of $NbFe_2$ consists of 4 f.u. and has a layered structure as shown in Fig. 1. One layer is formed by hexagonal sheet of Fe at site 6*h*. Another layer consists of Nb at site 4*f* and Fe at site 2*a*. The Nb atoms reside in Fe cages. Fe atoms at site 6*h* form Kagome lattice sheets as shown in Fig. 2. Therefore there are two types of Fe atoms, which may behave differently from a magnetic point of view. In the related compound, $TiFe_2$, neutron-scattering measurements have shown that Fe on the 6*h* sites form ferromagnetic sheets, which are stacked antiferromagnetically while there is no moment on the 2*a* Fe sites.[14] Furthermore, it has been reported that in that material there is a competition between ferromagnetic and antiferromagnetic ground states both from density-functional calculations and experimental measurements in samples with quenched disorder.[15,16] This indicates that the 2*a* site may play an important role in the magnetism of $TiFe_2$ even though it does not have ordered moments. It has been argued that the magnetic behaviors of the different C14 Laves TFe_2 compounds, where *T* is an early transition metal, are closely related,[17] and so one may conjecture that $NbFe_2$ is similar to $TiFe_2$. On the other hand, the presence of Kagome sheets in a material near a quantum critical point is suggestive of different physics since strong geometric frustration would be present if there were dominant near neighbor antiferromagnetic interactions in the sheets. In fact, the nature of magnetism at and in the vicinity of the quantum

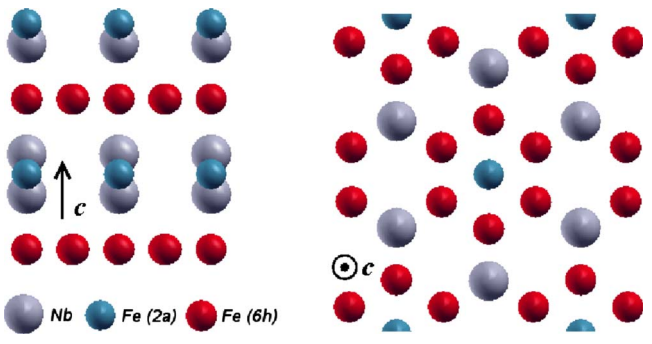

FIG. 1. (Color online) Crystal structure of $NbFe_2$ viewed along the *b* and *c* axes.

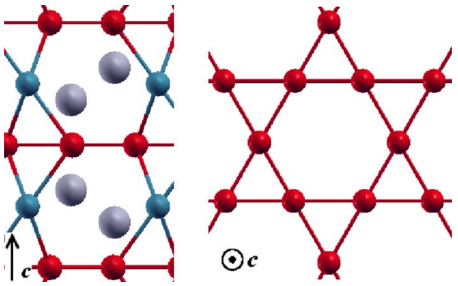

FIG. 2. (Color online) (Left) Crystal structure of $NbFe_2$ showing Nb atoms inside Fe cage. (Right) Kagome lattice layer formed by Fe at site 6*h*.

critical point is under debate. Further NMR studies have confirmed Yamada and Sakata's result[18–20] but neutron studies have not identified the magnetic order owing to very small magnetic moment and difficulty in growing clean single-crystal samples.[8,11] It has been presumed that the antiferromagnetism is of the spin-density wave type[18] but an explanation based on frustration of Fe layers with Kagome-type arrangement has also been proposed.[21] As $NbFe_2$ shows rich interplay of different type of magnetism within a small composition region, this system provides a good opportunity to study ferromagnetic quantum criticality and the precise nature of critical phenomena of the quantum critical point.

II. FIRST-PRINCIPLES CALCULATIONS

Here, we present the results of first-principles calculations on stoichiometric $NbFe_2$. Our electronic-structure calculations were performed within the local spin-density approximation (LSDA) using the general potential linearized augmented plane-wave (LAPW) method[22] as implemented in our in-house code. This is a full potential method with a flexible basis and no shape approximations to either the potential or charge density. The core states were treated relativistically while for the valence states a scalar relativisitic method was used. We used LAPW spheres of radii $2.2a_0$ for Nb and Fe. A well converged basis set with cutoff, $K_{max}=9.0/R_{min}$, where R_{min} is the minimum sphere radius was employed. Additional local orbitals were used to treat the Fe 3*s* and 3*p*, and Nb 4*s* and 4*p* states with the valence states. We used Brillouin-zone samplings derived from an $8\times8\times8$ grid for the self-consistent calculations and did tests with a doubled $16\times16\times16$ grid. The Fermi surfaces and densities of states shown were obtained using a $32\times32\times32$ grid of first-principles band energies. A denser interpolated $72\times72\times72$ grid based on the $32\times32\times32$ grid of first-principles data was used for the Lindhard function. We used the experimental lattice parameters, $a=4.838$ Å and $c=7.889$ Å,[23] but relaxed the atom positions in the unit cell. The calculated atomic position parameters were $x=0.0660$ and $y=0.1705$. For comparison, the experimental parameters are $x=0.0629$ and $y=0.1697$.

We find that magnetism of $NbFe_2$ is itinerant and obtain calculated moments that are much larger compared to experimental values. This type of error in which the LSDA overestimates the stability of magnetic states is uncommon but is

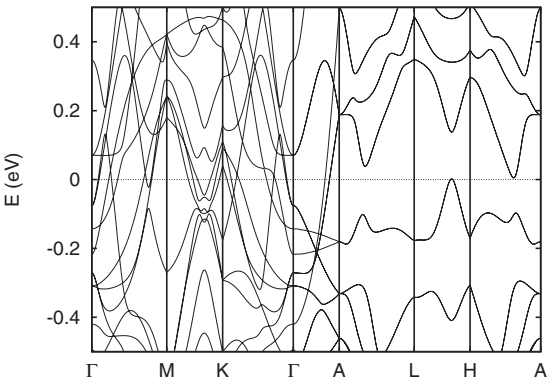

FIG. 3. Calculated band structure of nonspin-polarized $NbFe_2$. The Fermi energy is at 0 eV.

found generally in materials near magnetic quantum critical points. It indicates that the effect of beyond mean-field renormalizations (i.e., renormalization due to quantum spin fluctuations), which reduce the moment from the static LSDA value, is large. This type of renormalization of moments is also found in $ZrZn_2$ (Ref. 24) and Ni_3Al,[25] and indicates crucial role of spin fluctuations that are presumably associated with the QCP. In any case, the LSDA moments for $NbFe_2$ are found to depend on ordering and go to zero for some configurations, implying an itinerant nature for the magnetism. Furthermore, an analysis of the energetics shows that there are strong Fe-Fe interactions that compete with each other. Among the various magnetic ordering configurations we studied, we find ferrimagnetic ordering has the lowest energy. From a symmetry point of view ferrimagnetism is the same as ferromagnetism in that there is a net magnetization.

Our results for the electronic structure and density of states (DOS) without spin polarization are shown in Figs. 3 and 4, respectively. The general features of these are similar to the results obtained by Ishida *et al.*[26] using Koringa-Kohn-Rostoker (KKR) method. However, there are differences in the dispersion of bands and the band crossings at the Fermi level, presumably reflecting the use of shape approximations in the KKR methodology, as compared to the full potential LAPW approach. For example, the small Fermi surface at Γ is a hole section in our calculations but is a small electron

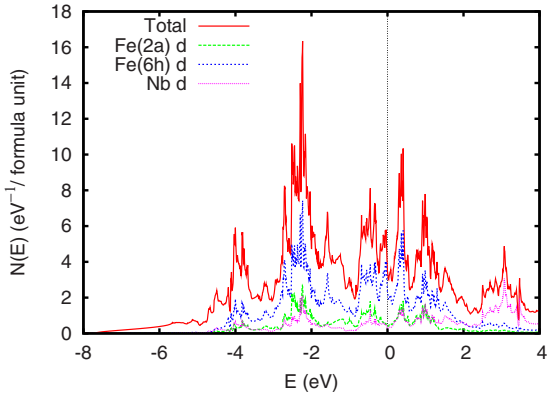

FIG. 4. (Color online) Electronic density of states of nonspin-polarized $NbFe_2$. The Fermi energy is at 0 eV.

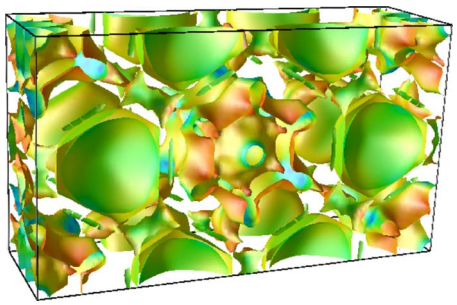

FIG. 5. (Color online) Fermi surface of nonspin-polarized $NbFe_2$. The figure contains two Brillouin zones and the shading is proportional to contribution of Fe at 6*h* site with red and blue indicating high and low values, respectively.

section in the KKR calculations. The electronic density of states of this material has also been calculated by Terao and Shimizu,[27] Takayama and Shimizu,[28] and Inoue and Shimizu.[29] These are qualitatively similar to our results but have different value for DOS at the Fermi energy. From the calculations, we find that most of the *s* and *p* bands lie well below Fermi level. The lowest three valence bands, starting at ~−8 eV with respect to E_F, are light and have mainly Fe *sp* character. The remaining bands above these are derived from mainly *d* orbitals of Nb and Fe. These bands are more flat as may be expected and give rise to peaks in DOS. The Fermi level lies near the bottom of one of these peaks with $N(E_F)=3.5$ eV^{-1} per formula unit both spins. Within Stoner theory,[30] a material has ferromagnetic instability when $NI>1$. Here N is the density of states at E_F on a per Fe per spin basis, $N=3.5/4$ eV^{-1} per Fe per spin. Using the typical value of $I\sim 0.7-0.9$ eV for Fe *d* electrons,[31,32] this gives a Stoner enhancement $(1-NI)^{-1}\sim 3$, which puts $NbFe_2$ away from a ferromagnetic Stoner instability (this is an instability where all Fe atoms polarize together) but still indicates significant renormalization and the possibility of ferromagnetic spin fluctuations. Furthermore the Fermi level lies near the bottom of a valley. The density of states increases strongly below E_F. Above E_F on a large scale (0.1 eV) the density of states is flat followed by a steep increase. Therefore hole doping will increase $N(E_F)$ and likely move the system closer to a ferromagnetic instability and more importantly disorder will increase the effective $N(E_F)$.

As may be seen, there are several bands crossing the Fermi energy. $NbFe_2$ has a large, three-dimensional (3D) and multisheet Fermi surface as shown in Fig. 5. The Fermi velocities are in fact rather isotropic, $v_{xx}=0.96\times 10^5$ m/s in plane and $v_{zz}=1.07\times 10^5$ m/s in the *c*-axis direction. This argues against explanations of the magnetic behavior based on two dimensionality. This also argues against explanations in terms of frustration on the two-dimensional (2D) Kagome sheets since the material is effectively 3D (also as discussed below, we do not find nearest-neighbor antiferromagnetism on the sheets, which again argues against this explanation).

Previous theoretical studies on the nature of magnetism in $NbFe_2$ have yielded disparate results. Ishida *et al.*[26] found that $NbFe_2$ does not fulfill Stoner condition and suggested a paramagnetic ground state. On the other hand, Asano and Ishida[33] calculated total energy as a function of lattice constant and magnetic moment, and found an antiferromagnetic state to have the lowest energy. However, they also found the antiferromagnetic state to be energetically close to two other type of ferromagnetic states.

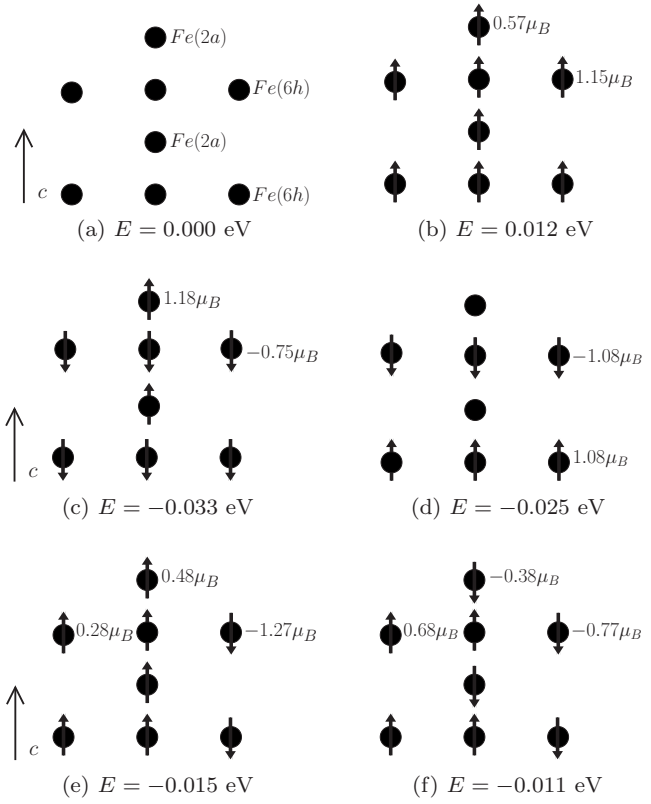

FIG. 6. Cartoons depicting various spin configurations of Fe in $NbFe_2$. Only Fe atoms are shown.

We did calculations for various spin configurations as shown in the cartoons in Fig. 6. We only studied collinear magnetic ordering cases and the direction of moment on each atom is indicated by an arrow. The cartoons also show the moments on Fe atoms as defined by the spin density within the Fe LAPW spheres. We have only shown Fe atoms in our cartoons as the induced moments on the Nb atoms were small compared to the moments on Fe atoms. The ground-state energy per unit cell is given relative to that of the nonspin-polarized case, which is shown in Fig. 6(a). Figure 6(b) illustrates the case when spins of all Fe atoms are aligned in the same direction. The moments on Fe 2*a* and 6*h* atoms are $0.57\mu_B$ and $1.15\mu_B$, respectively. The energy is +0.012 eV relative to the nonspin-polarized case. Hence, this configuration is energetically unfavorable and in fact is metastable with respect to the nonspin-polarized case. However, a state where the 6*h* and 2*a* sites have moments in opposite directions has the same symmetry and is more favorable. Figure 6(c) depicts this ferrimagnetic case. The energy of this state is −0.033 eV, which is also the lowest among all the orderings we studied. In this solution the moment on each 2*a* site is $1.18\mu_B$, while each 6*h* Fe has $0.75\mu_B$ in the opposite direction. The induced Nb moment is $0.09\mu_B$ in the same direction as the 2*a* site. This shows that there is a tendency toward moment formation on the 2*a* sites, in contrast to what might be surmised from the absence of an

ordered moment on this site in $TiFe_2$. However, the next lowest-energy state studied [Fig. 6(d)] does have zero moments on the 2*a* sites. In this configuration the 6*h* layers are stacked antiferromagnetically. The moments on the 2*a* sites converged to zero in this case, although we did not enforce this by symmetry and started self-consistent iterations with the 2*a* sites stacked along the *c* axis both ferromagnetically and antiferromagnetically with respect to each other (each 2*a* site is adjacent to an up-spin and a down-spin 6*h* layer in these calculations; the stacking we are referring to is the stacking of the 2*a* sublattice). The energy of this antiferromagnetic state is −0.025 eV with 6*h* moments of $1.08\mu_B$. This is the same ordering as was observed in $TiFe_2$.[14] The corresponding state with the 6*h* layers stacked ferromagnetically is the ferromagnetic state discussed above. As mentioned, it is high in energy and metastable against moment collapse to the nonspin-polarized state. This shows that there is a rather strong antiferromagnetic interaction between the stacked 6*h* layers if they are ferromagnetic in plane.

We also studied the possibility of frustration in the Kagome-type Fe 6*h* layers due to antiferromagnetic interactions. This was done by calculating configurations with spins flipped in the 6*h* sheets, as shown in Figs. 6(e) and 6(f). In both cases considered, the energy is negative relative to the nonspin-polarized case but well above the energies of the orderings in Figs. 6(c) and 6(d). This is opposite to what would occur if there were dominant antiferromagnetic interactions between neighbors in the Kagome sheets and so we conclude that this is not the case. Interestingly, these solutions with flipped spins in the 6*h* sites also showed significant moments on the 2*a* sites and furthermore depending on the stacking had very different moments on the different sites in the 6*h* layers.

We performed calculations on other orderings as well but they all either converged to the nonspin-polarized case or one of the previous configurations. These calculations show that the moments are strongly dependent on ordering and go to zero for some configurations. Hence, magnetism in this material is of itinerant type with an interplay between magnetic order and moment formation.

All the ordering patterns discussed above involve different spin arrangements within one unit cell (eight Fe atoms). As such they represent different branches at the Γ point. In order to extend this, we calculated the Lindhard susceptibility, $\chi_0(q,\omega)=\Sigma_k M_{k,k+q}\frac{f(\epsilon_k)-f(\epsilon_{k+q})}{\epsilon_k-\epsilon_{k+q}-\omega-i\delta}$, neglecting the matrix elements $M_{k,k+q}$, which we set to unity. Figure 7 shows the real part in the zero energy (static susceptibility) limit. We found only weak structure with peaks at the wave vectors $Q\sim(0.41,\ 0.97,\ 0.38)$, (0.69, 0.13, 0.38), (0.41, 0.97, 0.69), and (0.69, 0.13, 0.69). The value of $\chi_0(q)=1.23\times10^{-4}$ emu/mol at the peaks is comparable to $\chi_0(0)=1.13\times10^{-4}$ emu/mol. Therefore the nesting is not strong. Furthermore, we note that our neglect of the matrix element *M* in the Lindhard functions in general leads to an overestimate at finite *q* relative to Γ since the $M=1$ at Γ and $M\leq1$ at finite *q*.

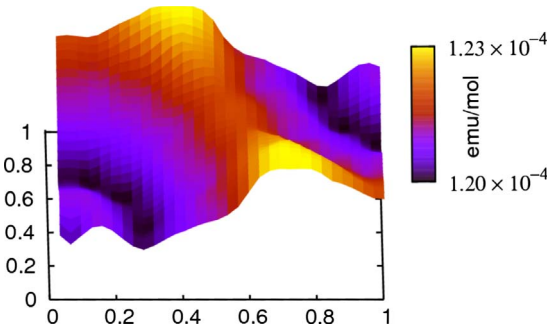

FIG. 7. (Color online) The real part of the Lindhard susceptibility $\chi_0(q,\omega\to0)$ for the plane $(q_x,q_y,0.38)$ that contains the maximum value. For comparison, the susceptibility for $q=(0,0,0)$ is $\chi_0(0)=1.13\times10^{-4}$ emu/mol.

III. DISCUSSION AND CONCLUSIONS

To summarize the main results of our calculations: (1) the magnetism of $NbFe_2$ is highly itinerant. The moments are dependent on ordering and go to zero for some configurations. Furthermore, some magnetic configurations are unstable with respect to the nonspin-polarized system, meaning that stable local moments do not exist. (2) There are strong magnetic interactions between Fe 2*a* and 6*h* layers. The interlayer 2*a*-2*a* and 6*h*-6*h* interactions are also strong. Ferrimagnetic ordering of Fig. 6(c) has lowest energy with largest moment on Fe(2*a*). However, the antiferromangetic ordering of Fig. 6(d) is almost degenerate with the ferrimagnetic state. This implies competing magnetic interactions. (3) There are not strong nearest-neighbor antiferromagnetic tendencies in the Kagome layers, and furthermore the electronic structure and magnetic interactions are three dimensional. This implies that geometric frustration based on antiferromagnetic interactions in the 2D Kagome planes is unlikely to be the main player in the quantum criticality. (4) The calculated Lindhard susceptibility shows only weak structure arguing against scenarios involving a simple spin-density wave. (5) The magnetic moments in our first-principles calculations are much too high compared to experiment. This implies that there is a substantial renormalization presumably due to spin fluctuations. As mentioned, this may be a signature of quantum fluctuations associated with a critical point, as was discussed for $ZrZn_2$ (Ref. 24) and Ni_3Al.[25] The characteristic of overestimated moments is also shared with the iron superconductors.[34]

It has been argued that large renormalizations generally occur in materials where there is a large phase space for spin fluctuations.[25,35–38] This follows from the fluctuation dissipation theorem, which relates the fluctuation amplitude to the energy and momentum integrated imaginary (dissipative) part of the susceptibility. Thus large amplitude fluctuations and renormalization are expected when the imaginary part of the susceptibility is large over an extended space. The imaginary part of the susceptibility is also what is measured in inelastic magnetic neutron scattering. Therefore, even though the ordered moments are very difficult to measure by neutron diffraction, important insights into the behavior of this material, specifically identification of competing magnetic states that may exist in relation to the quantum critical behavior may be obtained from inelastic scattering. If the LSDA moments represent mean-field values that are then reduced by fluctuations, the amplitude of these fluctuations must be siz-

able, and therefore they should be visible in experiments. It would be of considerable interest to perform such measurements. Finally, we mention one important difference between the iron superconductors and $NbFe_2$. In $NbFe_2$ ferrimagnetism, which from a symmetry point of view is ferromagnetism, is nearby both based on LSDA results and experimental data as a function of alloying. Crucially, ferromagnetic spin fluctuations are strongly pair breaking for singlet superconductivity.

ACKNOWLEDGMENT

This work was supported by the Department of Energy, Division of Materials Sciences and Engineering.

[1] R. B. Laughlin, G. G. Lonzarich, P. Monthoux, and D. Pines, Adv. Phys. **50**, 361 (2001).
[2] Y. Kamihara, T. Watanabe, M. Hirano, and H. Hosono, J. Am. Chem. Soc. **130**, 3296 (2008).
[3] I. I. Mazin, D. J. Singh, M. D. Johannes, and M. H. Du, Phys. Rev. Lett. **101**, 057003 (2008).
[4] M. V. Nevitt, C. W. Kimball, and R. S. Preston, Proceedings of the International Conference on Magnetism, Nottingham, 1964 (The Institute of Physics and The Physical Society, London, 1964), p. 137.
[5] Y. Yamada, Y. Kitaoka, K. Asayama, and A. Sakata, J. Phys. Soc. Jpn. **53**, 3198 (1984).
[6] Y. Yamada and A. Sakata, J. Phys. Soc. Jpn. **57**, 46 (1988).
[7] H. Wada, M. Hada, M. Shiga, and Y. Nakamura, J. Phys. Soc. Jpn. **59**, 701 (1990).
[8] M. Brando, D. Moroni-Klementowicz, C. Albrecht, and F. M. Grosche, Physica B **378-380**, 111 (2006).
[9] M. Brando, D. Moroni-Klementowicz, C. Albrecht, W. Duncan, D. Grüner, R. Boll, B. Fåk, and F. M. Grosche, J. Magn. Magn. Mater. **310**, 852 (2007).
[10] M. Brando, W. J. Duncan, D. Moroni-Klementowicz, C. Albrecht, D. Grüner, R. Ballou, and F. M. Grosche, Phys. Rev. Lett. **101**, 026401 (2008).
[11] D. Moroni-Klementowicz, M. Brando, C. Albrecht, W. J. Duncan, F. M. Grosche, D. Grüner, and G. Kreiner, Phys. Rev. B **79**, 224410 (2009).
[12] J. F. van Acker, Z. M. Stadnik, J. C. Fuggle, H. J. W. M. Hoekstra, K. H. J. Buschow, and G. Stroink, Phys. Rev. B **37**, 6827 (1988).
[13] F. Bondino, E. Magnano, M. Malvestuto, F. Parmigiani, M. A. McGuire, A. S. Sefat, B. C. Sales, R. Jin, D. Mandrus, E. W. Plummer, D. J. Singh, and N. Mannella, Phys. Rev. Lett. **101**, 267001 (2008).
[14] P. J. Brown, J. Deportes, and B. Ouladdiaf, J. Phys.: Condens. Matter **4**, 10015 (1992).
[15] E. Hoffmann, P. Entel, E. Wassermann, K. Schwarz, and P. Mohn, J. Phys. IV **5**, C2-117 (1995).
[16] J. Koble and M. Huth, Phys. Rev. B **66**, 144414 (2002).
[17] S. Ishida, S. Asano, and J. Ishida, J. Phys. Soc. Jpn. **54**, 4695 (1985).
[18] Y. Yamada, H. Nakamura, Y. Toke, K. Asayama, K. Koga, A. Kati, and T. Murakami, J. Phys. Soc. Jpn. **59**, 2976 (1990).
[19] M. R. Crook and R. Cywinski, J. Magn. Magn. Mater. **140-144**, 71 (1995).
[20] M. Kurisu, Y. Andoh, and Y. Yamada, Physica B **237–238**, 493 (1997).
[21] M. R. Crook and R. Cywinski, Hyperfine Interact. **85**, 203 (1994).
[22] D. J. Singh and L. Nordstrom, *Planewaves, Pseudopotentials and the LAPW Method*, 2nd ed. (Springer, Berlin, 2006).
[23] B. S. Bokshtein, N. P. D'Yakonova, G. S. Nikol'skii, and Y. D. Yagodkin, Russ. J. Phys. Chem. **51**, 1273 (1977).
[24] I. I. Mazin and D. J. Singh, Phys. Rev. B **69**, 020402(R) (2004).
[25] A. Aguayo, I. I. Mazin, and D. J. Singh, Phys. Rev. Lett. **92**, 147201 (2004).
[26] S. Ishida, S. Asano, and J. Ishida, J. Phys. Soc. Jpn. **54**, 3925 (1985).
[27] K. Terao and M. Shimizu, Phys. Status Solidi B **139**, 485 (1987).
[28] N. Takayama and M. Shimizu, J. Phys. F: Met. Phys. **18**, L83 (1988).
[29] J. Inoue and M. Shimizu, J. Magn. Magn. Mater. **79**, 265 (1989).
[30] E. C. Stoner, Proc. R. Soc. London **169**, 339 (1939).
[31] O. K. Andersen, J. Madsen, U. K. Poulsen, O. Jepsen, and J. Kollar, Physica B & C **86-88**, 249 (1977).
[32] U. K. Poulsen, J. Kollar, and O. K. Andersen, J. Phys. F: Met. Phys. **6**, L241 (1976).
[33] S. Asano and S. Ishida, J. Phys.: Condens. Matter **1**, 8501 (1989).
[34] I. I. Mazin, M. D. Johannes, L. Boeri, K. Koepernik, and D. J. Singh, Phys. Rev. B **78**, 085104 (2008).
[35] T. Moriya, *Spin Fluctuations in Itinerant Electron Magnetism* (Springer, Berlin, 1985).
[36] A. Z. Solontsov and D. Wagner, Phys. Rev. B **51**, 12410 (1995).
[37] A. Ishigaki and T. Moriya, J. Phys. Soc. Jpn. **67**, 3924 (1998).
[38] P. Larson, I. I. Mazin, and D. J. Singh, Phys. Rev. B **69**, 064429 (2004).